文章编号: 1001 - 2060(2016) 05 - 0082 - 06

煤层厚度对煤岩体内热 - 流耦合传热的影响

杨　伟, 曹　明, 赵柄翔, 张美琳
(辽宁工程技术大学 建筑工程学院, 辽宁 阜新 123000)

摘　要: 根据现场煤层厚度的多样性, 构建关于煤体、岩体及煤岩体(煤岩高度比为 1:2, 1:1, 2:1) 的热 - 流耦合传热的数学模型; 考虑测得孔隙度、颗粒直径、阻力影响及温度加载方式, 引入局部热平衡假设和 Brinkman-Darcy-Forchheimer 建立守恒方程组, 进行数值求解, 将计算结果与实验进行对比。研究表明: 煤岩体中央处对流作用最弱, 近壁面处流体对流作用最强, 流体经过煤岩接触面处速度发生突变; 随煤岩体中煤层增厚, 流函数最大值 $|\psi|_{max}$ 减小, 对流换热能力减弱; 在传热过程中, 流场与温度场的规律相对应, 随瑞利数 Ra 增大, $\overline{Nu}$ 呈指数增加趋势。通过验证, 地温与暴露立侧面风流温差在 10 ~ 30 ℃时, 该模拟能很好的预测煤层厚度对热流耦合传热规律产生的影响。为有效预防煤层自燃、岩体损伤力学分析及煤矿能源合理露采等提供科学依据。

关　键　词: 煤层厚度; 多孔介质; 煤岩体; 热 - 流耦合

中图分类号: TD313; TD727　　**文献标识码:** A

DOI: 10.16146/j.cnki.rndlgc.2016.05.012

引　言

基于煤岩工程不断深入发展, 煤岩力学发展的方向已不局限于对煤体、岩体的研究, 煤矿安全生产, 资源合理的开采利用等工程实践对煤系地层煤岩体的研究提出了更高要求。对此, 国内外学者相继开展许多关于煤与顶底板岩层力学性质随温度、煤岩高度比变化规律的研究: 王晓楠对不同高度比的煤岩组合体进行试验研究, 得到了高度比对受载破坏中声发射和微震效应的影响规律[1]; Heuze、Alshayea 及查文华等人先后通过实验及模拟手段对岩体力学特性分析, 指出了其力学性质受温度影响[2~4]; 何江等人研究了煤岩高度比对力学抗压强度的影响关系[5]; 邓绪彪等人模拟了煤岩厚度对发生冲击灾害时煤岩体结构破坏的影响[6]; 杨永明等人揭示温度对岩石宏观力学性能及微观孔隙结构演化规律的影响机理[7]; Petukhov 和 Linkov 最早提出了两体系统并分析了煤岩体系统的稳定性[8]; 窦林名等人通过对顶板 - 煤体 - 底板所构成的组合煤岩体进行试验究, 指出冲击矿压危险性与煤岩体高度比的密切关系[9]; 杨伟等研究低温裂隙 - 孔隙流对高温裂隙岩石的温度场影响[10]; 李小璐等人对变煤岩高度比进行模拟, 分析煤岩体不同的组合模式对冲击倾向性的影响[11]; Schneider, Combarnous, Seki 等人发现多孔介质本身结构特性不仅影响岩体力学性质[12~14], 对热 - 流耦合传热过程也产生重要影响。

目前, 研究主要集中在上述参数对煤岩体力学性能影响等方面, 而现存关于煤岩体结构特性对内部热 - 流耦合传热影响的研究相对较少, 基于由温度分布、传热所引起的矿井热害、煤层自燃、煤系岩石损伤和变形破坏等煤岩工程灾害考虑, 开展结构特性对煤岩体传热影响的研究具有重要指导意义, 本文侧重研究高度比。

本研究在前人研究结果基础上, 根据现场实况并基于多孔介质多场耦合传热等理论, 考虑煤岩体骨架的内部阻力、颗粒直径、孔隙率、渗透率及流体粘性阻力, 建立控制方程, 数值计算煤矿开采中煤岩体热量传递情况, 得到高度比对煤岩体传热机理影响规律。

1　物理模型

1.1　煤岩体物理模型

内蒙古准格尔新鑫露天矿位于鄂尔多斯市的东胜煤田勃牛川普查区外围的东北部, 矿区开采标高

收稿日期: 2015 - 04 - 17;　修订日期: 2015 - 12 - 03
基金项目: 辽宁省大学生创新创业训练计划资助项目(201410147019); 国家自然科学基金资助项目(51274109)
作者简介: 杨　伟(1965 -), 男, 辽宁阜新人, 辽宁工程技术大学副教授.
通讯作者: 曹　明(1989 -), 女, 辽宁大石桥人, 辽宁工程技术大学硕士研究生.

1 310 ~ 1 260 m(最大垂直温差约为 1.465 ℃) 。开采境界分 3 个采区: 6 - 1 煤层平均煤厚 1.96 m,6 - 2 煤层平均煤厚 3.33 m,6 - 3 煤层平均煤厚 4.46 m。鉴于当地冬冷夏热,地温与风流温差随季节性变化剧烈。经实地调研,矿区内煤质以长焰煤为主,处于烟煤煤化程度 I 阶段,变质程度低,易自燃; 顶底板岩性以砂岩为主,透水性好,为地下水贮存和运移提供了条件,故可认为模型内部充满水,简化煤层构造如图 1 所示。

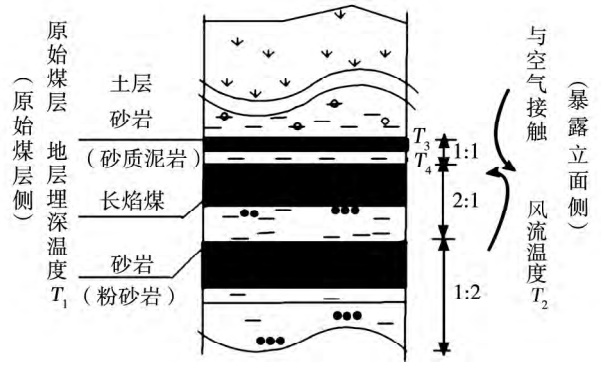

图 1　煤层构成简图

Fig. 1 Sketch showing the composition of the coal bed

根据矿区内可采煤层厚度不同,故建立煤岩体时需考虑煤岩高度比例对传热影响。煤体选用矿区长焰煤,岩体选取该煤层附近的砂岩,煤岩体物理模型从煤岩接触面处抽取,接触面上下两侧的煤岩高度比例按考察煤矿的实际赋存比例(1∶2,1∶1,2∶1) 选取,建立长 × 高为 H(m) × H(m) 的煤岩体模型,其中,固体骨架按多孔介质考虑,内部充满水,如图 1 所示。边界条件按组合台阶式开采所产生的煤岩右侧露头的赋存状态建立,即模型右侧边界为暴露面温度 $T2$ 侧,左侧边界为地温 $T1$ 侧,由于上、下边界与其相邻层紧邻,无温差,热量传递为零,故绝热处理($\partial t/\partial n = 0$) 。重力影响按煤岩高度比例考虑,重力加速度 g 方向取 y 轴负方向。鉴于该区风流温度与地温温差随季节性变化[15],及当地埋深每增加 100 m,温度增高 2.93 ℃[16],需考虑不同温度加载方式($\Delta t = |T_1 - T_2|$) 及温度随埋深变化对热 - 流耦合传热影响。由于无论上下边界温度随埋深如何变化,均与相邻层无热量传递,即埋深对初始边界的影响仅表现为由 T_1 导致的 Δt 的改变($\Delta t = |T_1 - T_2|$, $T_1 = (T_3 + T_4)/2$,其中 T_3 、T_4 为上、下边界温度) ,故按 Δt = 10、20、30 ℃ 考虑。下面以高度比为 1∶1 的煤岩体模型为例,如图 2 所示。

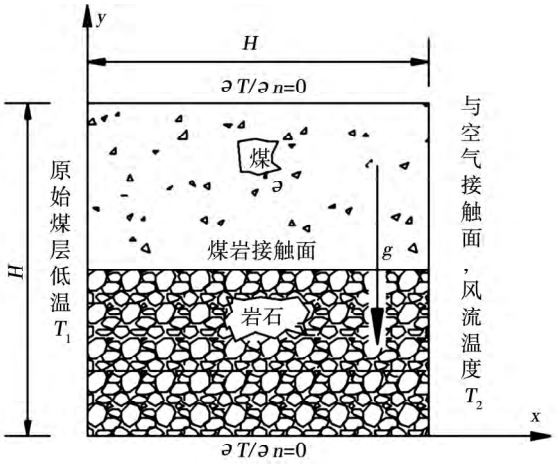

图 2　物理模型

Fig. 2 Physical model

2　数学方程

2.1　控制方程

多孔介质内流体流动换热遵循三个守恒方程,其微分方程表示为连续性方程、动量方程和能量方程。对连续性方程式(1) 采用非稳态表达形式; 模型壁面采用速度无滑移条件,对 x、y 方向动量方程式(2) 、式(3) 采用 Brinkman 修正,对流速采用 Forchheimer 修正; 因流体流速大小约为 $10^{-6} \sim 10^{-4}$ m/s,流体固体间热交换充分,流体、固体温度相等,能量方程式(4) 采用局部热平衡假设,即 $T_f = T_s = T$,建立方程组如下:

连续性方程:

$$\phi \frac{\partial \rho_f}{\partial t} + \frac{\partial(\rho_f u)}{\partial x} + \frac{\partial(\rho_f v)}{\partial y} = 0 \tag{1}$$

x 方向动量方程:

$$\frac{\rho_f}{\phi}\frac{\partial u}{\partial t} + \frac{\rho_f}{\phi^2}\left[u\frac{\partial u}{\partial x} + v\frac{\partial u}{\partial y}\right] + \frac{1}{\phi}\frac{\partial(P\phi)}{\partial x} = \frac{\mu}{\phi}\left[\frac{\partial^2 u}{\partial x^2} + \frac{\partial^2 u}{\partial y^2}\right] - \frac{\mu}{K}u - C\frac{\rho_f}{\sqrt{K}}\sqrt{u^2 + v^2}\,u \tag{2}$$

y 方向动量方程:

$$\frac{\rho_f}{\phi}\frac{\partial v}{\partial t} + \frac{\rho_f}{\phi^2}\left[u\frac{\partial v}{\partial x} + v\frac{\partial v}{\partial y}\right] + \frac{1}{\phi}\frac{\partial(\phi P)}{\partial y} = \frac{\mu}{\phi}\left[\frac{\partial^2 v}{\partial x^2} + \frac{\partial^2 v}{\partial y^2}\right] - \frac{\mu}{K}v - C\frac{\rho_f}{\sqrt{K}}\sqrt{u^2 + v^2}\,v + (\rho_0 - \rho_f)g \tag{3}$$

能量方程:

$$[\phi(\rho c_p)_f + (1-\varphi)(\rho c)_s]\frac{\partial T}{\partial t} + (\rho c_p)_f\left[u\frac{\partial T}{\partial x} + v\frac{\partial T}{\partial y}\right] = [\phi k_f + (1-\phi)k_s]\left[\frac{\partial^2 T}{\partial x^2} + \frac{\partial^2 T}{\partial y^2}\right] \quad (4)$$

式中: C—无量纲阻力常数, $C = 1.75 \cdot 180^{-1/2} \cdot \phi^{-3/2}$; K—煤岩体渗透率, $K = \overline{d_s}^2 \cdot \phi^3 \cdot 180^{-1}(1-\phi)^{-2}$; 其它变量,如表 1 所示。

表 1 符号说明

Tab. 1 Explanations to the symbols

符号	名称	单位
ϕ	孔隙率	–
ρ / ρ_0	密度/参考密度	kg/m^3
u / v	x/y 方向流速	m/s
P	压力	Pa
t	时间	s
T	热力学温度	k
μ	有效粘度	Pa/s
g	重力加速度	m/s^2
c_p	水的定压比热容	J/(kg·k)
k	导热系数	W/(m·k)
$\overline{d_s}$	煤岩体平均颗粒直径	m
下标 s/f	固体/流体	–
下标 h/c	高温/低温	–

为揭示多孔介质内牛顿流体流动换热的普遍规律,上述方程采用无量纲控制方程表达形式。引入无量纲量定义: 无量纲坐标 $X = xH^{-1}$、$Y = yH^{-1}$; 无量纲速度 $U = uH\alpha^{-1}$、$V = vH\alpha^{-1}$; 无量纲压力 $p = PH^2\rho^{-1}\alpha^{-2}$; 无量纲密度 $\rho' = \rho\rho_0^{-1}$; 无量纲时间, $\tau = t\alpha H^{-2}$; 无量纲准则达西数 $Da = KH^{-2}$; 无量纲温度 $\theta = (T - T_c)(T_h - T_c)^{-1}$, 下标 h、c—高温、低温; 普朗特数 $Pr = \nu\alpha^{-1}$; ν—运动粘度, m^2/s; 定义 $Ra = g\beta|T_h - T_c|H^3\nu^{-1}\alpha^{-1}$ 为瑞利数; α—多孔介质的热扩散系数, m^2/s; T—任一点温度值, k。式(1)~式(4)转化为无量纲形式为:

连续性方程:

$$\frac{\partial(\phi\rho')}{\partial\tau} + \frac{\partial(\rho' U)}{\partial X} + \frac{\partial(\rho' V)}{\partial Y} = 0 \quad (5)$$

x 方向动量方程:

$$\frac{1}{\phi}\frac{\partial U}{\partial\tau} + \frac{1}{\phi^2}\left[U\frac{\partial U}{\partial X} + V\frac{\partial U}{\partial Y}\right] + \frac{1}{\phi}\frac{\partial(\phi p)}{\partial X} = \frac{Pr}{\phi}\left[\frac{\partial^2 U}{\partial X^2} + \frac{\partial^2 U}{\partial Y^2}\right] - \frac{Pr}{Da}U - C\frac{\sqrt{(U^2+V^2)}}{\sqrt{Da}}U \quad (6)$$

y 方向动量方程:

$$\frac{1}{\phi}\frac{\partial V}{\partial\tau} + \frac{1}{\phi^2}\left[U\frac{\partial V}{\partial X} + V\frac{\partial V}{\partial Y}\right] + \frac{1}{\phi}\frac{\partial(\phi p)}{\partial Y} = \frac{Pr}{\phi}\left[\frac{\partial^2 V}{\partial X^2} + \frac{\partial^2 V}{\partial Y^2}\right] - \frac{Pr}{Da}V - C_F\frac{\sqrt{(U^2+V^2)}}{\sqrt{Da}}V + RaPr\theta \quad (7)$$

能量方程:

$$\frac{\phi(\rho c_p)_f + (1-\phi)(\rho c)_s}{(\rho c_p)_f}\cdot\left[\frac{\partial\theta}{\partial\tau} + U\frac{\partial\theta}{\partial X} + V\frac{\partial\theta}{\partial Y}\right] = \frac{(1-\phi)k_s + \varepsilon k_f}{(\rho c_p)_f}\cdot\left[\frac{\partial^2\theta}{\partial X^2} + \frac{\partial^2\theta}{\partial Y^2}\right] \quad (8)$$

2.2 定解条件

初始条件为:

$\tau = 0$, $U = V = 0$, $\theta = 0$。

无量纲边界条件为:

$\tau > 0$, $Y = 0$, $Y = H$, $U = V = 0$, $\partial\theta/\partial n = 0$; $X = 0$, $U = V = 0$, $\theta = 1$;

$X = 1$, $U = V = 0$, $\theta = 0$。

局部努塞尔数:

$$Nu = \frac{(\partial T/\partial n)_{wall}H}{Th - Tc} = \left.\frac{\partial\theta}{\partial n}\right|_{wall} \quad (9)$$

高温壁面平均努塞尔数定义为:

$$\overline{Nu} = \frac{1}{H}\int_0^H Nu\,dy = -\frac{1}{H}\int_0^H\left(\frac{\partial T}{\partial X}\right)_{x=0}dy \quad (10)$$

2.3 模型验证

建立煤岩高度比例为 1∶2,1∶1,2∶1 的煤岩体,以 $\Delta t = 10$ ℃为例,其它实验条件同图 2 所示。对煤岩接触面上下 5 cm 处分别设置 8 个温度测点,由图 3 可知: 高度比越大,即煤层越厚,接触面上下温差越小,越不利于热量传递。从实验结果观察,与模拟值基本一致,从而完成数值模拟与实验的相互验证。

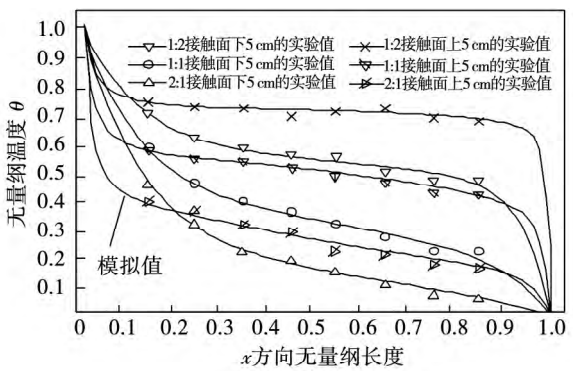

图 3 实验值与模拟值对比

Fig. 3 Contrast of the test values and the simulation ones

3　结果和分析

3.1　高度比对温度场和流场影响

本研究主要针对 Ra 从 100 到 1 000 变化时,通过改变高度比例,分析流动传热产生的影响。实测煤、岩孔隙率及煤体平均颗粒直径得: $\phi_{岩石}$ = 0.068 7, $\phi_{煤}$ = 0.121 8; $\bar{d}_{煤}$ = 0.001 m, $\bar{d}_{岩石}$ = 0.001 m[17]; 以下取煤岩高度例比为 1∶2,1∶1,2∶1; Δt = 10 ℃; Ra 为 500 的计算结果为例,如图 4 所示。

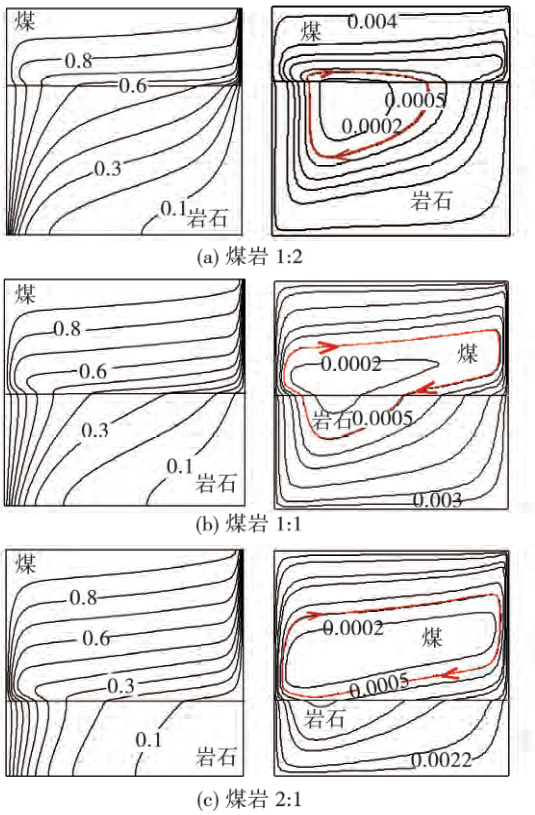

(a) 煤岩 1:2

(b) 煤岩 1:1

(c) 煤岩 2:1

图 4　无量纲温度(左)、流线分布图(右)

Fig. 4 Chart showing the distribution of dimensionless temperature (Left) and streamline (Right)

图 4 为煤岩体变高度比例对应的无量纲温度、流线分布图,图中细线为煤岩体接触面。从无量纲温度图可知: 温度由煤岩体高温边界到低温边界方向均匀降低。随煤层增厚,煤体内高温壁面下侧及低温壁面上侧等温线变密,即导热热流密度变大,导热作用增强; 岩体内左侧高温壁面下侧及低温壁面上侧等温线变稀疏,即导热热流密度减小,导热作用减弱; 在煤岩体中,低温边界上侧对流换热强度与高温边界下侧对流换热作用变化趋势相反。

从流线随煤岩体变高度比分布图可以看出: 流体在煤岩体内部呈顺时针流动,流函数数值从中间区域向边界增加,腔体内部流动最弱,边界流动最强。随煤层增厚,煤单体内高、低温边界两侧流线变密,流动加剧,则对流换热作用增强; 但岩单体内高温和低温壁面流线变稀疏,流动减缓,对流换热作用减弱; 整个煤岩体区域流函数最大值 $|\psi|_{max}$ 随煤层增厚而减小; 流体在经过煤岩接触面速度矢量处发生突变; 整个传热过程中,流场与温度场相对应。

3.2　不同煤层厚度下高温边界 $\overline{Nu}$ 随 Ra 变化

为描述煤层厚度变化时高温边界 $\overline{Nu}$ 随 Ra 变化的函数关系,将离散数据公式化。观察五组离散数据呈非线性增加趋势,故对其采用非线性曲线拟合。经比较,不同温差下,指数型拟合曲线的拟合精度最高,达 99.9% 以上,拟合公式如下:

$$Nu = ARa^{B} \tag{11}$$

具体参数值及各公式的拟合优度如表 2 ~ 表 4 所示,与不同加载温度下的拟合曲线一一对应,如图 5(a)、(b)、(c) 所示。

表 2　Δt = 10 ℃ 时拟合参数

Tab. 2 Parameters fitted when Δt = 10 ℃

高度比例	A	B	拟合优度/%
岩体	0.473 99	0.615 19	99.943
煤岩 1:2	0.431 20	0.529 21	99.993
煤岩 1:1	0.352 45	0.512 89	99.965
煤岩 2:1	0.236 40	0.528 41	99.971
煤体	0.045 76	0.622 42	99.953

表 3　Δt = 20 ℃ 时拟合参数

Tab. 3 Parameters fitted when Δt = 20 ℃

高度比例	A	B	拟合优度/%
岩体	0.853 37	0.615 94	99.937
煤岩 1:2	0.769 51	0.529 45	99.993
煤岩 1:1	0.632 32	0.512 33	99.968
煤岩 2:1	0.443 38	0.521 35	99.980
煤体	0.082 03	0.623 8	99.948

观察图 5 可知,不同温差下,当 Ra 由 100 变化到 1 000 时,高温边界 $\overline{Nu}$ 随 Ra 变化曲线均呈现指数增加趋势; Δt 从 10 ℃ 变化到 30 ℃ 过程中,温差

越大，$\overline{Nu}$ 越大；温差一定时，$\overline{Nu}_{岩体} > \overline{Nu}_{煤岩1:2} > \overline{Nu}_{煤岩1:1} > \overline{Nu}_{煤岩2:1} > \overline{Nu}_{煤体}$。即温差越大，换热效果越好；温差一定时，岩体热流耦合换热能力优于煤体，且煤层越厚，煤岩体换热效果越差。

表 4 $\Delta t = 30$ ℃时，拟合参数

Tab. 4 Parameters fitted when $\Delta t = 30$ ℃

高度比例	A	B	拟合优度/%
岩体	0.898 52	0.615 94	99.937
煤岩 1:2	0.810 47	0.529 4	99.992
煤岩 1:1	0.665 12	0.512 47	99.970
煤岩 2:1	0.469 81	0.520 45	99.981
煤体	0.086 36	0.623 8	99.948

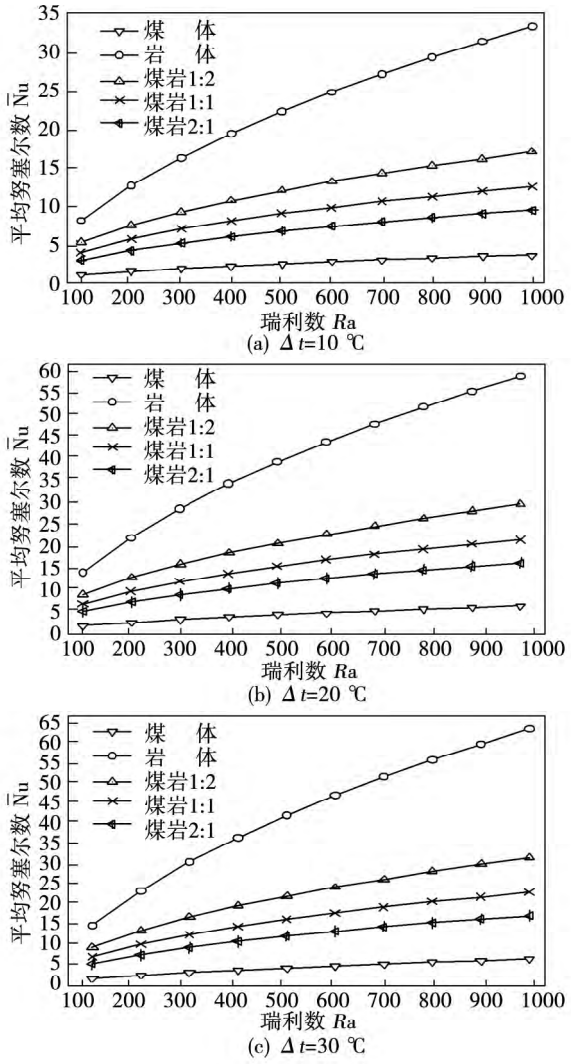

图 5 高温边界 $\overline{Nu}$ 随 Ra 变化曲线

Fig. 5 Variation curves of $\overline{Nu}$ at the high temperature boundary lines with Ra

3.3 规律推广

为排除自然界中，因煤岩两种介质上下位置因素对煤岩体传热规律的干扰，揭示煤层厚度对煤岩体传热影响规律的普适性，防止因埋深不同导致的边界条件 $T_1 = (T_3 + T_4)/2$ 无法与原始模型比较，故选取同一标高处，构建岩体在上、煤体在下物理模型，边界条件设置如图 2 所示。对比煤岩介质上下位置不同时的煤岩体内部流动传热情况，并选取煤岩体高度比例为 1:4 和 4:1 作为辅助论证，当 $\Delta t = 10$ ℃，如图 6、图 7 所示。经数值验证，当 Ra 从 100 到1 000变化时，无量纲温度场、流场，及 $\overline{Nu}$ 变化与前文结果完全吻合，均严格遵从煤层厚度对煤岩体热－流耦合传热影响的规律，阐明论文结果可靠性。

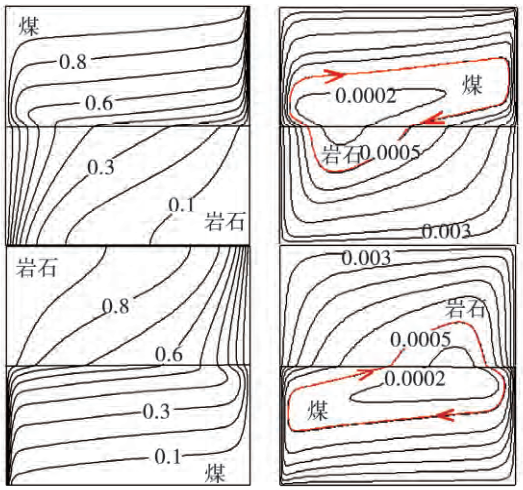

图 6 无量纲温度(左)、流线分布图(右)

Fig. 6 Chart showing the distribution of dimensionless temperature (Left) and streamline (Right)

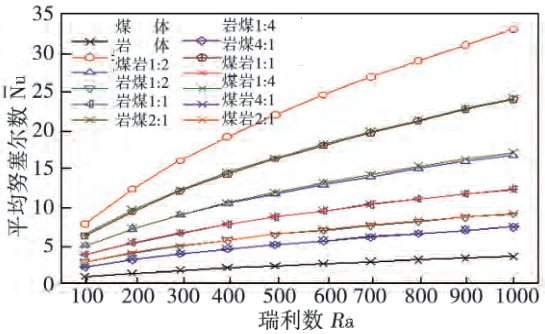

图 7 高温边界 $\overline{Nu}$ 随 Ra 变化曲线

Fig. 7 Variation curves of $\overline{Nu}$ at the high temperature boundary lines with Ra

4 结　论

(1) 随着煤岩体中煤层增厚,煤体内高、低温边界导热作用均增强; 岩体内高、低温边界导热作用均减弱; 煤岩体整体的高温边界下侧导热减弱,低温边界上侧导热增强,变化趋势与单体物质内高、低温边界导热作用变化趋势相反;

(2) 随着煤岩体中煤层增厚,煤岩体 $\overline{Nu}$ 减小,换热能力减弱; 煤岩体与煤体、岩体相比较时,岩体高温边界处 $\overline{Nu}$ 明显大于煤岩体 $\overline{Nu}$,煤岩体 $\overline{Nu}$ 明显大于煤体 $\overline{Nu}$,即岩体换热能力优于煤体; 且煤层越厚,煤岩体换热效果越差;

(3) 随着煤岩体中煤层增厚,煤体内高、低温边界流动加剧; 岩体内高、低温壁面流动减缓; 煤岩体整体孔隙度变大,阻力减小,但 $|\psi|_{max}$ 减小,流动减缓,即热流耦合作用是造成岩体内流动强度大于煤体内流动强度的直接原因。

本研究得出的煤层厚度对煤岩体传热影响规律为防止煤层自燃,矿井热害,露天矿及深井矿中温度对煤系岩石损伤和变形破坏等损伤力学分析,保障合理露采及地热资源的开采等提供参考依据,对指导煤岩工程安全生产,合理制定露采方案及能源利用等提供参考。

参考文献:

[1] 王晓楠,陆菜平,薛俊华,等. 煤岩组合体冲击破坏的声发射及微震效应规律试验研究特征研究 [J]. 岩土力学,2011,32(5):1287 – 1296.
WANG Xiao-nan,LU Cai-ping,XUE Jun-hua,et al. Experimental research of the law governing the acoustic emission and microseismic effects caused by a shock destruction from a coal and rock-combined body and study of their characteristics [J]. Rock and Soil Mechanics,2011,32(5):1287 – 1296.

[2] Heuze F E. High-temperature mechanical,physical and thermal properties of granitic rocks-a review [J]. International Journal of Rock Mechanics and Mining Sciences & Geomechanics Abstracts,1983,20(1):3 – 10.

[3] Alshayea N A. Khan K. Abduljauward S N. Effects of confining pressure and temperature on mixed-mode (Ⅰ – Ⅱ) fracture toughness of a limestone rock [J]. International Journal of Rock Mechanics & Mining Sciences,2000,37(4):629 – 643.

[4] 查文华,宋新龙,武腾飞,等. 温度对煤系泥岩力学特征影响的试验研究 [J]. 岩土力学,2014,35(5):1334 – 1339.
ZHA Wen-hua,SONG Xin-long,WU Teng-fei,et al. Experimental study of the influence of temperature on the mechanical characteristics of coal-related mudstone [J]. Rock and Soil Mechanics,2014,35(5):1334 – 1339.

[5] 何　江,窦林名,陆菜平,等. 薄煤层冲击矿压特性及防治研究 [J]. 煤炭学报,2012,37(7):1094 – 1098.
HE Jiang,DOU Lin-ming,LU Cai-ping,et al. Study of the pressure characteristics of ores impinged by a thin coal bed and its prevention [J]. Journal of Coal,2012,37(7):1094 – 1098.

[6] 邓绪彪,胡海娟,徐　刚,等. 两体岩石结构冲击失稳破坏的数值模拟 [J]. 采矿与安全工程学报,2012,29(6):833 – 839.
DENG Xu-biao,HU Hai-juan,XU Gang,et al. Numerical simulation of the impingement and stability-loss destruction of a kind of dual-body rock structure [J]. Journal of Mining & Safety Engineering,2012,29(6):833 – 839.

[7] 杨永明,鞠　杨,陈佳亮,等. 温度作用对孔隙岩石介质力学性能的影响 [J]. 岩土工程学报,2013,35(5):856 – 864.
YANG Yong-ming,JU Yang,CHEN Jia-liang,et al. Influence of the action of temperature on the mechanical performance of porous rock media [J]. Journal of Rock and Soil Engineering,2013,35(5):856 – 864.

[8] Petukhov I M,Linkov A M. The theory of post-failure deformations and the problem of stability in rock mechanics [J]. International Journal of Rock Mechanics and Mining Sciences and Geomechanics,1979,16(5):57 – 76.

[9] 窦林名,陆菜平,牟宗龙,等. 组合煤岩冲击倾向性特性试验研究 [J]. 采矿与安全工程学报,2006,23(1):43 – 46.
DOU Lin-ming,LU Cai-ping,MU Zong-long,et al. Experimental study of the impingement tendency characteristics of combined coal and rocks [J]. Journal of Mining & Safety Engineering,2006,23(1):43 – 46.

[10] 杨　伟,杨秋实,杜　宝,等. 裂隙岩体渗流耦合传热分析 [J]. 中国地质灾害与防治学报,2012,23(1):99 – 102.
YANG Wei,YANG Qiu-shi,DU Bao,et al. Analysis of the coupled heat transfer of a seepage from fractured rocks [J]. Journal of Geological Disaster and Control in China,2012,23(1):99 – 102.

[11] 李晓璐,康立军,李宏艳,等. 煤 – 岩组合体冲击倾向性三维数值试验分析 [J]. 煤炭学报,2011,36(12):2064 – 2067.
LI Xiao-lu,KANG Li-jun,LI Hong-yan,et al. Analysis of the impingement tendency of a coal and rock combined body during a three-dimensional numerical test [J]. Journal of Coal,2011,36(12):2064 – 2067.

[12] Schneider,K,J. Proc. 11th Intl Congr [C]. Pergamon. 1963,Ⅱ(4):247.

[13] Combarnous,M. Convection naturelle et convection mixte en milieu poreux [D]. University of Paris,1970.

[14] Seki,N.,Fukusako,S. &Inaba,H. Transient behaviors of natural convec-tive heat transfer through a vertical porous layer [J]. Heat Mass Transfer 21. 1978,985.

[15] 于　强,任战利. 鄂尔多斯盆地黄陵、东胜地区地温场对比 [J]. 吉林大学学报(地球科学版),2008,38(6):933 – 945.
YU Qiang,REN Zhan-li. Contrast of the geothermal fields in Huangling and Dongsheng regions,Ordos Basin [J]. Journal of Jilin University (Geoscience Edition),2008,38(6):933 – 945.

[16] 张　盛. 鄂尔多斯盆地古地温演化与多种能源矿产关系的研究 [D]. 西安: 西北大学,2006.
ZHANG Sheng. Research of the relationship between the paleogeothermal evolution and several energy source mining capacity in Ordos basin [D]. Xi'an: Northwest University,2006.

[17] 赵阳升. 多孔介质多场耦合作用及其工程响应 [M]. 北京: 科学出版社,2010:1 – 2.
ZHAO Yang-sheng. Multi-field coupling action played by porous media and its engineering response [M]. Beijing: Science Press,2010:1 – 2.

(刘　瑶　编辑)

plated before and after the microbe foul test had a relatively small change, thus the coat surface thus prepared by using Ni-P alloy can effectively prohibit or reduce the weight of the microbe fouls and exhibit a relatively good foul-resistant effectiveness and erosion-resistant property, **Key words:** surface denaturing, chemically plated, Ni-P alloy, microbe foul, erosion-resistant property

制备新型高温受热面防磨涂层的实验研究 = Experimental Study of the Preparation of a New Type High-temperature Heating Surface Abrasion-preventive Coating [刊, 汉] QIANG Xue-cai, GUO Lin, WANG Hong-liang (CSIC Harbin No. 703 Research Institute, Harbin, China, Post Code: 150078) //Journal of Engineering for Thermal Energy & Power. -2016, 31(5). -76~81

An abrasion-resistant composite coat on the heating surface of a boiler made by using commonly-used steal material T91 was prepared by adopting the supersonic electric arc spraying technology, A bonding strength test, XRD analysis and high temperature erosion test of the coat under discussion were conducted. The test results show that the new type composite coat boasts an excellent high temperature erosion-resistant performance, thus applicable for protection of high temperature heating surfaces in boilers. **Key words:** supersonic electric arc spraying, bonding strength, XRD analysis; high temperature erosion

煤层厚度对煤岩体内热-流耦合传热的影响 = Study of the Influence of the Thickness of a Coal Bed on the Heat-flow Coupled Heat Transfer Inside Coal Rock Masses [刊, 汉] YANG Wei, CAO Ming, ZHAO Bing-xiang, ZHANG Mei-lin (College of Architectural Engineering, Liaoning Engineering Technology University, Fuxin, China, Post Code: 123000) //Journal of Engineering for Thermal Energy & Power. -2016, 31(5). -82~87

According to the diversity of the thickness of coal bed at the site, established was a heat-flow coupling model for coal, rock and coal-rock masses (the ratio of coal and rock height was 1:2, 1:1 and 2:1), With the porosity and particle diameter measured, resistance influence and temperature loading modes being taken into consideration as well as the local heat balance assumption and Brinkman-Darcy-Forchheimer model being introduced, a conservation equation group was established to seek a numerical solution, contrast and analyze the calculation results and the test ones. It has been found that the action of convection in the central part of the coal-rock mass is weakest and that nearing the wall surface is strongest. An abrupt change of the flow speed of the fluid passing through the contact surface of the coal and rock mass occurs. With an increase of the coal bed thickness in the coal-rock mass, the maximum value of the flow function $|\psi|_{max}$ will decrease and the ability of the convection-based heat exchange will be-

come weakened. In the heat transfer process, the flow field will correspond to the temperature one. With an increase of Ra number, $\overline{Nu}$ will assume an ascending tendency of the exponent. It has been verified that when the temperature difference between the ground temperature and the air flow temperature ranges from 10 ℃ to 30 ℃, the simulation method in question can predict very well the influence of the thickness of coal bed on the law governing the heat-flow coupling heat transfer, therefore offering a scientific basis for an effective prevention of spontaneous combustion in coal beds, an analysis of any damage to rock masses in mechanics and a rational surface mining of coal mines etc. **Key words:** coal bed thickness, porous medium, coal rock mass, heat-flow coupling

水蒸气和二氧化碳对金属载氧体抗积碳特性的影响 = Influence of Steam and Carbon Dioxide on the Carbon Deposition Characteristics of Metal Oxygen Carriers [刊,汉] HU Qiang, JIN Jing, XIONG Zhi-bo, WANG Yong-zhen (College of Energy Source and Power Engineering, Shanghai University of Science and Technology, Shanghai, China, Post Code: 200093) //Journal of Engineering for Thermal Energy & Power. -2016, 31(5). -88~92

In the light of the problem that carbon deposited on the surface of a metal oxygen carrier in a chemical chain combustion process will affect its activity, with the help of a small-scale test rig, studied were the carbon deposition characteristics of two kinds of metal oxygen carrier (Ni and Fe based) prepared at various reaction temperatures (650 ℃, 750 ℃, 850 ℃ and 950 ℃) in different reaction atmospheres (CH_4 and $CO + H_2$) by using the mechanical mixing method and probed was the inhibition action of steam or carbon dioxide added on the carbon deposition process of metal oxygen carriers during their reduction reactions. It has been found that in both reaction atmospheres, the carbon deposition phenomena to various extents will occur to the metal oxygen carriers, however, in the $CO + H_2$ atmosphere, the amount of carbon deposited is relatively small and an addition of steam or carbon dioxide can obviously inhibit the carbon deposited on the surface of the metal oxygen carriers and in the CO atmosphere, an addition of steam can totally remove the carbon deposited on the surface of metal oxygen carriers. The XRD (X-ray diffraction) analytic results further show that an addition of steam or carbon dioxide can effectively inhibit the production of carbon deposited on the surface of metal oxygen carriers and the inhibition effectiveness of steam is superior to that of carbon dioxide. **Key words:** chemical chain combustion, metal oxygen carrier, carbon deposition characteristics, steam

基于主成分分析的煤粉流动性实验研究 = Experimental Study of the Flowability of Pulverized Coal Based on an Analysis of the Principal Components [刊,汉] ZHANG Yue, QIAO Xiao-lei, LIU Hai-yu, JIN Yan (Col-